

## Real-Space Evidence of Trimeric, Tetrameric, and Pentameric Uracil Clusters Induced by Alkali Metals

Yuanqi Ding, Xinyi Wang, Donglin Li, and Wei Xu\*

Cite This: *J. Phys. Chem. C* 2020, 124, 5257–5262

Read Online

ACCESS |



Metrics &amp; More

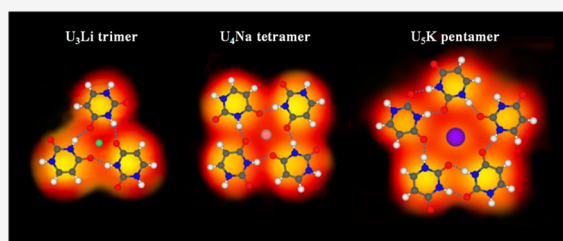


Article Recommendations



Supporting Information

**ABSTRACT:** Alkali metal cations are known as the significant participants in biological processes and play the vital role in nucleic acid structures. The interactions between alkali metals and nucleobases have therefore attracted a lot of attention. As a peculiar nucleobase in RNA, uracil with its magic number clusters induced by alkali metals has attracted tremendous interest over the past decades. Here, from the interplay of high-resolution scanning tunneling microscopy imaging and density functional theory calculations, we show the real-space evidence of the formation of trimeric, tetrameric, and pentameric uracil clusters induced by alkali metals (Li, Na, and K) on the Au(111) surface, and further investigate their specific configurations at the atomic-scale, which would be of importance for understanding the formation process of biologically relevant nanostructures involving cations *in vivo*.



## INTRODUCTION

Alkali metals, generally cationized in the cellular environments, are known as significant participants in several biological processes and play a vital role in some nucleic acid structures, such as inhibiting the chain initiation process by RNA polymerases and stabilizing nucleobase quartets within the telomere.<sup>1,2</sup> These functions of alkali metals are realized by interacting with negatively charged phosphate groups and nucleic acid bases through the electrostatic interaction, which further affects the syntheses, replication, and structural integrity of DNA and RNA.<sup>3–5</sup> Therefore, the interactions between alkali metals and nucleobases are significant and have attracted a lot of attention.<sup>6–20</sup> Among others, extensive studies reported that alkali metals, specifically lithium (Li), sodium (Na), and potassium (K), can significantly increase self-aggregation of the nucleobases and lead to the formation of uniquely stable magic number clusters,<sup>8,9,16,17,19</sup> such as the well-studied guanine (G) quartet stabilized by Na or K,<sup>21–25</sup> uracil (U) and thymine (T) quintets stabilized by K,<sup>26</sup> etc. These biologically relevant complexes with the magical aggregation number have potential in forming sophisticated nanostructures, whose configuration and stability are thus fundamentally important in different disciplines.<sup>27,28</sup> As a peculiar nucleobase in RNA, uracil with its magic number clusters induced by alkali metals has attracted tremendous interest over the past decades with theoretical investigations<sup>12–15,17,18</sup> and spectroscopy studies<sup>16,19,20</sup> performed in solution and gas phase. The G clusters induced by alkali metals have been successfully introduced to the surface science community and extensively studied by scanning tunneling microscopy (STM),<sup>22–25</sup> which provides atomic-scale structural information. Thus, it is of utmost interest to construct a

system of uracil and alkali metals under well controlled ultrahigh vacuum (UHV) conditions with the aim of potentially forming series of uracil clusters on the surface, and further providing real-space structural evidence at the atomic scale.

Herein, we choose U molecules and alkali metals Li, Na and K, together with the noble Au(111) surface as a model system to explore the fundamental interactions between U molecules and alkali metals. The Au(111) surface is employed as a template to ensure that the molecules adopt flat adsorption geometries to facilitate the potential formation of the potential U-M clusters (where M denotes Li, Na, and K, respectively). From the interplay of high-resolution STM imaging and density functional theory (DFT) calculations, we show that the formation of U–Li trimers, U–Na tetramers, and U–K pentamers stabilized by a combination of hydrogen bonds and electrostatic ionic interactions is achieved on the Au(111) surface (cf. Scheme 1). This systematic study demonstrates the feasibility on the formation of magic number U clusters and moreover allows us to explore the fundamental interactions between U molecules and alkali metals in real space.

## EXPERIMENTAL AND THEORETICAL METHODS

All STM experiments were performed in a UHV chamber (base pressure  $1 \times 10^{-10}$  mbar) equipped with a variable-

Received: January 8, 2020

Revised: February 7, 2020

Published: February 7, 2020

Scheme 1. Schematic Illustration on the Formation of Trimeric, Tetrameric, Pentameric Uracil Clusters Induced by Alkali Metals (Li, Na, and K) on the Au(111) Surface

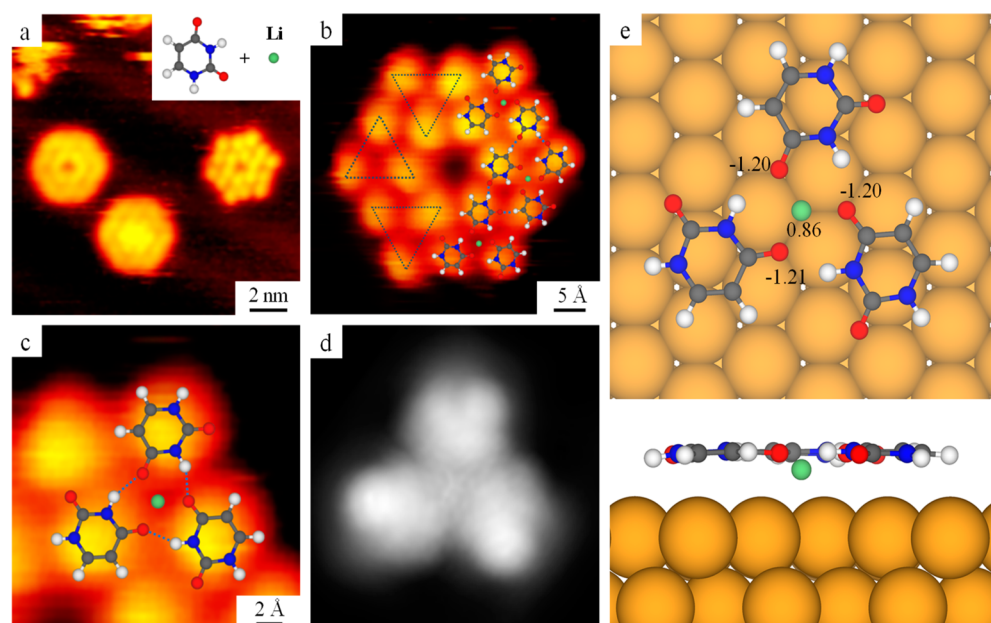
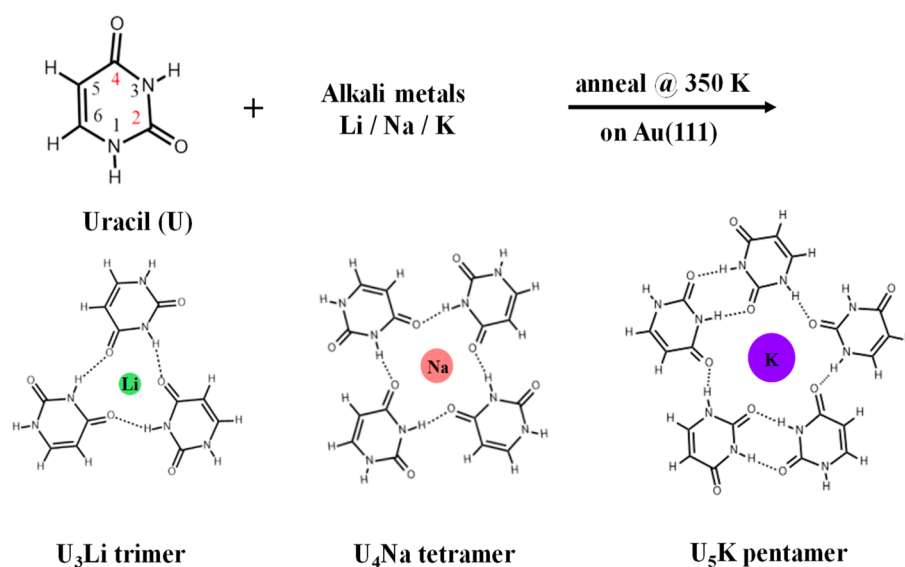


**Figure 1.** Formation of the hexagonal structure composed of the U<sub>3</sub>Li trimers after deposition of U and Li on the Au(111) surface followed by annealing at 350 K. (a) A large-scale STM image showing the discretely distributed hexagonal structures. (b) A close-up STM image allows the elementary building blocks as depicted by blue triangles to be distinguished. The superimposed DFT-optimized model shows the interconnections between the U<sub>3</sub>Li trimers via hydrogen bonds. (c) A high-resolution zoom-in STM image of the U<sub>3</sub>Li trimer superimposed with the DFT-optimized model on Au(111) (the substrate is omitted for clear presentation). Hydrogen bonds are depicted by blue dashed lines. (d) The simulated STM image of the U<sub>3</sub>Li trimer at a bias voltage of 1.7 V. (e) Top and side views of the DFT-optimized structural model of the U<sub>3</sub>Li trimer on Au(111) with the bader charge analysis of Li and O. Au, yellow; H, white; C, gray; N, blue; O, red; Li, green. Scanning conditions:  $I_t = 1.2$  nA,  $V_t = 1.7$  V.

temperature, fast-scanning “Aarhus-type” STM using electrochemically etched W tips purchased from SPECS,<sup>29,30</sup> a molecular evaporator and an e-beam evaporator, and other standard instrumentation for sample preparation. The Au(111) substrate was prepared by several cycles of 1.5 keV Ar<sup>+</sup> sputtering followed by annealing to 800 K for 15 min, resulting in clean and flat terraces separated by monatomic steps. The Uracil molecule (purchased from Sigma-Aldrich, purity >98%) was loaded into the glass crucible in the molecular evaporator. After a thorough degassing, the molecules are deposited onto

the Au(111) surface by thermal sublimation. The alkali metals lithium and sodium were evaporated from Alvasource (from Alvattec), and potassium was evaporated from alkali metal dispensers (from SAES) via conventional resistance heating after fully degassing. The sample was thereafter transferred within the UHV chamber to the STM, where measurements were carried out at ~100–150 K. All of the STM images were further smoothed to eliminate noises.

The calculations were performed in the framework of DFT by using the Vienna ab initio simulation package (VASP).<sup>31,32</sup>

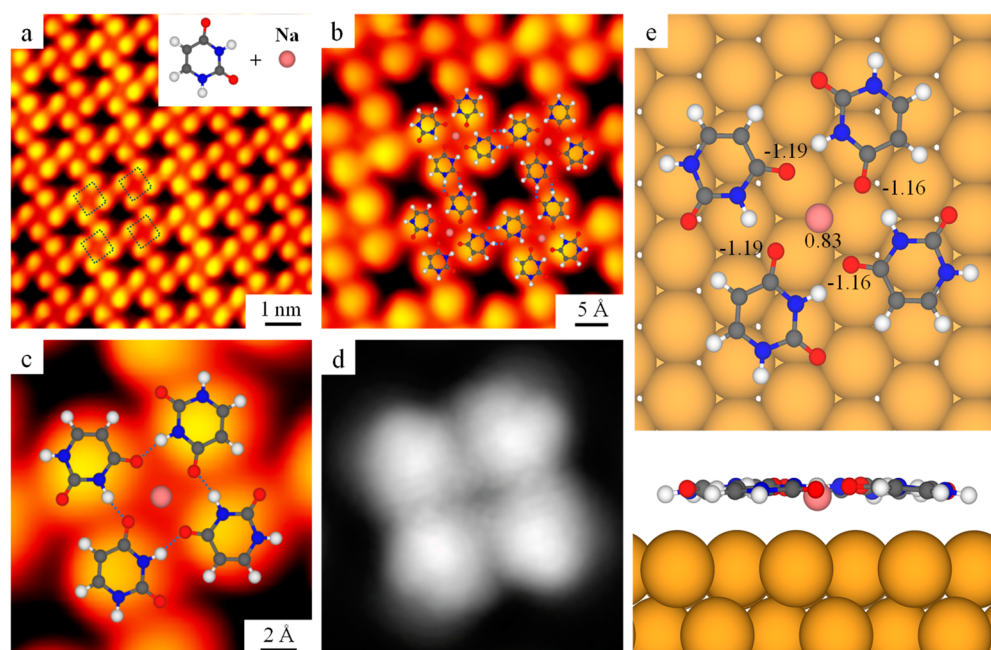


**Figure 2.** Formation of the network structure composed of the  $U_4Na$  tetramers after deposition of U and Na on the Au(111) surface followed by annealing at 350 K. (a) A large-scale STM image showing the network structure composed of  $U_4Na$  tetramers as depicted by the blue squares. (b) A close-up STM image allows the elementary  $U_4Na$  tetramer building blocks to be distinguished with the superimposed DFT-optimized model. (c) A high-resolution zoom-in STM image of the  $U_4Na$  tetramer superimposed with the DFT-optimized model on Au(111) (the substrate is omitted for clear presentation). Hydrogen bonds are depicted by blue dashed lines. (d) The simulated STM image of the  $U_4Na$  tetramer at a bias voltage of 1.2 V. (e) Top and side views of the DFT-optimized structural model of the  $U_4Na$  tetramer on Au(111) with the bader charge analysis of Na and O. Au, yellow; H, white; C, gray; N, blue; O, red; Na, pink. Scanning conditions:  $I_t = 0.9$  nA,  $V_t = 1.2$  V.

The projector-augmented wave method was used to describe the interaction between ions and electrons,<sup>33,34</sup> the Perdew–Burke–Ernzerhof generalized gradient approximation (GGA) exchange–correlation functional was employed,<sup>35</sup> and van der Waals interactions were included using the dispersion-corrected DFT-D3 method of Grimme.<sup>36</sup> The atomic structures were relaxed using the conjugate gradient algorithm scheme as implemented in the VASP code until the forces on all unconstrained atoms were  $\leq 0.03$  eV/Å. The simulated STM images were obtained by the Hive program based on the Tersoff–Hamann method.<sup>37,38</sup>

## RESULTS AND DISCUSSION

Deposition of U molecules and metal Li at a low surface coverage (ca. 0.2 monolayer) on the Au(111) surface followed by annealing at 350 K leads to the formation of the hexagonal structures which are discretely distributed on the surface (Figure 1a). It is reported previously that U molecules form a close-packed self-assembled structure on the Au(111) surface,<sup>39–41</sup> without any structure transformation on Au(111) after annealing at 350 K as showing in our experiment (Figure S1). The hexagonal structure thus results from the interactions between U and Li by forming a metal–organic structure. The close-up STM image (Figure 1b) reveals that the hexagonal structure is composed of triangular clusters (depicted by blue triangles). The cluster shows three bright protrusions and a dim center (more clearly resolved in Figure S2). Theoretical studies<sup>13,14,20</sup> showed that alkali metals prefer to interact with the uracil molecule at the O4 site (cf. Scheme 1, the single U molecular model). Based on the above analysis, we performed DFT calculations to build up the atomic-scale model on the triangular cluster. From the high-resolution zoom-in STM image and the superimposed structural model shown in Figure

1c, we then attribute the triangular cluster to a  $U_3Li$  trimer, in which the central Li interacts with U molecules via electrostatic ionic bonds, and the neighboring U molecules are linked with each other by  $NH\cdots O$  hydrogen bonds (depicted by blue dashed lines). The corresponding simulated STM image (Figure 1d) shows a good agreement with the experimental one. From the superimposed DFT-optimized model in Figure 1b, we identify that the  $U_3Li$  clusters are linked with the adjacent ones via the  $CH\cdots O$  and  $NH\cdots O$  hydrogen bonds between U molecules (depicted by blue dashed lines). Moreover, Bader charge analysis of the  $U_3Li$  cluster on Au(111) is performed as shown in Figure 1e. As seen, the central Li is positively charged (in a +0.86 charged state), and the three O atoms are all negatively charged (in around  $-1.2$  charged states), which confirms the electrostatic ionic interactions between Li and O within the  $U_3Li$  cluster.

Interestingly, if we change the alkali metal from Li to Na, deposition of U molecules and Na on the Au(111) surface followed by annealing at 350 K leads to the formation of a metal–organic network structure as shown in Figure 2a. From the STM image, we identify that such a network is composed of the quadrilateral clusters as depicted by the blue squares. Closer inspection of the network (Figure 2b) shows that the square motif is formed by four bright protrusions and a dim central spot, which are attributed to U molecules and Na cation, respectively. Note that the central Na cation can be visible in a special tip state, as illustrated in Figure S3. From the high-resolution zoom-in STM image and the superimposed structural model shown in Figure 2c, we then attribute the square motif to a  $U_4Na$  tetramer, in which the central Na interacts with U molecules via electrostatic ionic bonds, and the neighboring U molecules are linked with each other by  $NH\cdots O$  hydrogen bonds (depicted by blue dashed lines). The

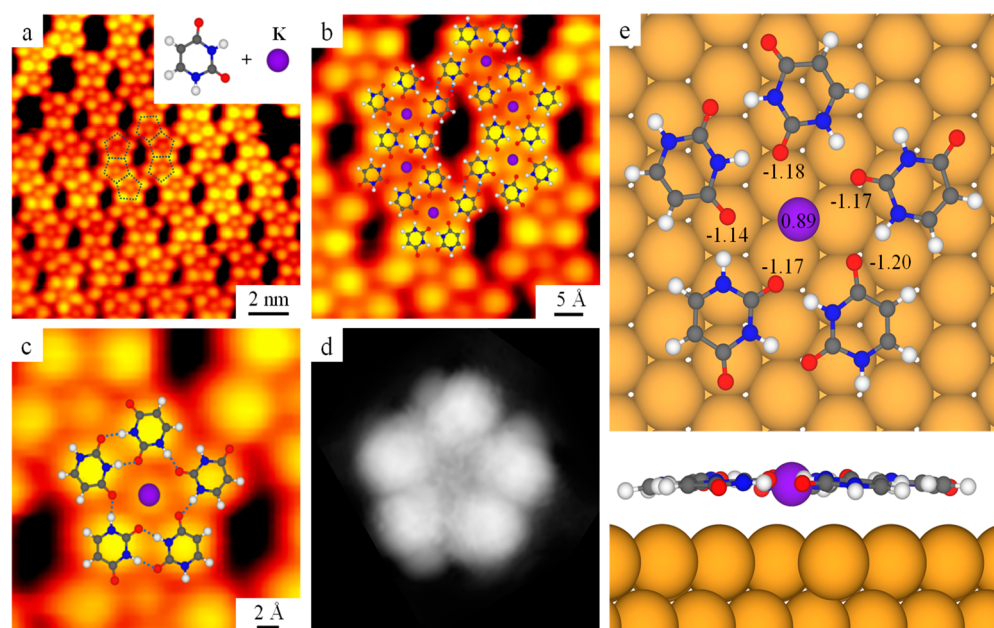


**Figure 3.** Formation of the metal–organic network structure composed of the  $U_5K$  pentamer after deposition of K and U on the Au(111) surface followed by annealing at 350 K. (a) A large-scale STM image showing the network structure composed of  $U_5K$  pentamers as depicted by the blue pentagons. (b) A close-up STM image with the superimposed DFT-optimized model allows to distinguish the elementary  $U_5K$  pentamer building blocks and their hydrogen bonding interconnections. (c) A high-resolution zoom-in STM image of the  $U_5K$  pentamer superimposed with the DFT-optimized model on Au(111) (the substrate is omitted for clear presentation). Hydrogen bonds are depicted by blue dashed lines. (d) The simulated STM image of the  $U_5K$  pentamer at a bias voltage of 1.4 V. (e) Top and side views of the DFT-optimized structural model of the  $U_5K$  motif on Au(111) with the bader charge analysis of K and O. Au, yellow; H, white; C, gray; N, blue; O, red; K, purple. Scanning conditions:  $I_t = 0.8$  nA,  $V_t = 1.4$  V.

corresponding simulated STM image is shown in Figure 2d. From the superimposed network model in Figure 2b, we identify that the  $U_4Na$  tetramers are linked with the adjacent ones via two  $NH\cdots O$  hydrogen bonds between U molecules (depicted by blue dashed lines). Moreover, Bader charge analysis of the  $U_4Na$  cluster on Au(111) is performed as shown in Figure 2e. The central Na is positively charged as  $+0.83 e^-$  and the four O atoms are all negatively charged as  $-1.2 e^-$  confirming the electrostatic ionic interactions between Na and O within the  $U_4Na$  cluster.

A step further, if we change the alkali metal from Na to K, deposition of U molecules and K on the Au(111) surface followed by annealing at 350 K leads to the formation of a metal–organic network structure composed of the pentagonal clusters as shown in Figure 3a. Closer inspection of the STM image with the superimposed structural models (Figure 3b,c) shows that the pentagon motif is formed by five U molecules and a K cation, which is then attributed to a  $U_5K$  metal–organic motif, where the central K cation is normally visible. The same as  $U_3Li$  and  $U_4Na$  motifs, within the  $U_5K$  one, the central K interacts with U molecules via electrostatic ionic bonds, and the neighboring U molecules are linked with each other by  $NH\cdots O$  hydrogen bonds (depicted by blue dashed lines). The corresponding simulated STM image of  $U_5K$  motif is shown in Figure 3d. From the superimposed network model in Figure 3b, we identify that each  $U_5K$  pentamer shares two U dimers with the adjacent ones on both sites to form one-dimensional chains, and the chains are linked together laterally by double  $NH\cdots O$  hydrogen bonds between U molecules (depicted by blue dashed lines). The Bader charge analysis of the  $U_5K$  cluster on Au(111) is performed as shown in Figure 3e. The central K is positively charged as  $+0.89 e^-$  and the five

O atoms are all negatively charged as  $-1.2 e^-$  confirming the electrostatic ionic interactions between K and O within the  $U_5K$  cluster.

## CONCLUSION

In conclusion, by the combination of STM imaging and DFT calculations, we have presented the real-space experimental evidence on the formation of  $U_3Li$  trimer,  $U_4Na$  tetramer, and  $U_5K$  pentamer on Au(111), in which the size of metal cations is an important factor for determining the formation and stability of metal–organic motifs with different aggregation numbers. Such a systematic study may help to increase our fundamental understandings on the function and effect of alkali metals to nucleic acids, and moreover provide a method to form the metal–organic clusters with controllable aggregation numbers on surfaces.

## ASSOCIATED CONTENT

### Supporting Information

The Supporting Information is available free of charge at <https://pubs.acs.org/doi/10.1021/acs.jpcc.0c00188>.

STM image showing the close-packed structure after deposition of pure uracil on Au(111) followed by annealing to 350 K without addition of any alkali metal; a close-up STM image with exaggerated contrast to show the dim center of  $U_3Li$  cluster; a high-resolution STM image in special tip state where the Na ions are resolved (PDF)

## AUTHOR INFORMATION

## Corresponding Author

Wei Xu – Interdisciplinary Materials Research Center, College of Materials Science and Engineering, Tongji University, Shanghai 201804, P. R. China; [orcid.org/0000-0003-0216-794X](https://orcid.org/0000-0003-0216-794X); Email: [xuwei@tongji.edu.cn](mailto:xuwei@tongji.edu.cn)

## Authors

Yuanqi Ding – Interdisciplinary Materials Research Center, College of Materials Science and Engineering, Tongji University, Shanghai 201804, P. R. China

Xinyi Wang – Interdisciplinary Materials Research Center, College of Materials Science and Engineering, Tongji University, Shanghai 201804, P. R. China

Donglin Li – Interdisciplinary Materials Research Center, College of Materials Science and Engineering, Tongji University, Shanghai 201804, P. R. China

Complete contact information is available at: <https://pubs.acs.org/10.1021/acs.jpcc.0c00188>

## Notes

The authors declare no competing financial interest.

## ACKNOWLEDGMENTS

The authors acknowledge financial support from the National Natural Science Foundation of China (21622307 and 21790351) and the Fundamental Research Funds for the Central Universities. Aidi Zhao is acknowledged for providing the Li and Na sources.

## REFERENCES

- (1) Hsiao, C.; Tannenbaum, E.; VanDeusen, H.; Hershkovitz, E.; Perng, G.; Tannenbaum, A. R.; Williams, L. D. Complexes of Nucleic Acids with Group I and II Cations. In *Nucleic Acid-Metal Ion Interactions*; Hud, N. V., Ed.; Royal Society of Chemistry: Cambridge, U.K., 2009; pp 1–38.
- (2) Aoki, K.; Murayama, K. Nucleic Acid-Metal Ion Interactions in the Solid State. In *Interplay between Metal Ions and Nucleic Acids*; Sigel, A., Sigel, H., Sigel, R. K. O., Eds.; Springer: Dordrecht, 2012; pp 43–102.
- (3) Sigel, H. Interactions of Metal-Ions with Nucleotides and Nucleic-Acids and Their Constituents. *Chem. Soc. Rev.* **1993**, *22*, 255–267.
- (4) Kaim, W.; Schwedersky, B. *Bioinorganic Chemistry: Inorganic Elements in the Chemistry of Life*; John Wiley & Sons: Chichester, 1994; pp 7–15.
- (5) Nakano, S.; Fujimoto, M.; Hara, H.; Sugimoto, N. Nucleic acid duplex stability: influence of base composition on cation effects. *Nucleic Acids Res.* **1999**, *27*, 2957–2965.
- (6) Burda, J. V.; Šponer, J.; Hobza, P. Ab Initio Study of the Interaction of Guanine and Adenine with Various Mono- and Bivalent Metal Cations ( $\text{Li}^+$ ,  $\text{Na}^+$ ,  $\text{K}^+$ ,  $\text{Rb}^+$ ,  $\text{Cs}^+$ ;  $\text{Cu}^+$ ,  $\text{Ag}^+$ ,  $\text{Au}^+$ ;  $\text{Mg}^{2+}$ ,  $\text{Ca}^{2+}$ ,  $\text{Sr}^{2+}$ ,  $\text{Ba}^{2+}$ ,  $\text{Zn}^{2+}$ ,  $\text{Cd}^{2+}$ , and  $\text{Hg}^{2+}$ ). *J. Phys. Chem.* **1996**, *100*, 7250–7255.
- (7) Lee, G.-Y. DFT studies of the lithium complexes of DNA bases. *Bull. Korean Chem. Soc.* **2002**, *23*, 1023–1026.
- (8) Gu, J. D.; Leszczynski, J. Isoguanine complexes: Quintet versus tetrad. *J. Phys. Chem. B* **2003**, *107*, 6609–6613.
- (9) Meyer, M.; Sühnel, J. Self-association of isoguanine nucleobases and molecular recognition of alkaline ions: Tetrad vs pentad structures. *J. Phys. Chem. A* **2003**, *107*, 1025–1031.
- (10) Hashemianzadeh, S. M.; Faraji, S.; Amin, A. H.; Ketabi, S. Theoretical Study of the Interactions between Isolated DNA Bases and Various Groups IA and IIA Metal Ions by Ab Initio Calculations. *Monatsh. Chem.* **2008**, *139*, 89–100.

(11) Gillis, E. A. L.; Fridgen, T. D. The hydrated  $\text{Li}^+$ -adenine-thymine complex by IRMPD spectroscopy in the N–H/O–H stretching region. *Int. J. Mass Spectrom.* **2010**, *297*, 2–8.

(12) Cerda, B. A.; Wesdemiotis, C.  $\text{Li}^+$ ,  $\text{Na}^+$ , and  $\text{K}^+$  binding to the DNA and RNA nucleobases. Bond energies and attachment sites from the dissociation of metal ion-bound heterodimers. *J. Am. Chem. Soc.* **1996**, *118*, 11884–11892.

(13) Rodgers, M. T.; Armentrout, P. B. Noncovalent interactions of nucleic acid bases (uracil, thymine, and adenine) with alkali metal ions. Threshold collision-induced dissociation and theoretical studies. *J. Am. Chem. Soc.* **2000**, *122*, 8548–8558.

(14) Russo, N.; Toscano, M.; Grand, A. Bond energies and attachment sites of sodium and potassium cations to DNA and RNA nucleic acid bases in the gas phase. *J. Am. Chem. Soc.* **2001**, *123*, 10272–10279.

(15) Russo, N.; Toscano, M.; Grand, A. Lithium affinity for DNA and RNA nucleobases. The role of theoretical information in the elucidation of the mass spectrometry data. *J. Phys. Chem. B* **2001**, *105*, 4735–4741.

(16) Koch, K. J.; Aggerholm, T.; Nanita, S. C.; Graham Cooks, R. Clustering of nucleobases with alkali metals studied by electrospray ionization tandem mass spectrometry: implications for mechanisms of multistrand DNA stabilization. *J. Mass Spectrom.* **2002**, *37*, 676–686.

(17) Meyer, M.; Sühnel, J. Interaction of cyclic cytosine-, guanine-, thymine-, uracil- and mixed guanine-cytosine base tetrads with  $\text{K}^+$ ,  $\text{Na}^+$  and  $\text{Li}^+$  ions—a density functional study. *J. Biomol. Struct. Dyn.* **2003**, *20*, 507–517.

(18) Zhu, W.; Luo, X.; Puah, C. M.; Tan, X.; Shen, J.; Gu, J.; Chen, K.; Jiang, H. The multiplicity, strength, and nature of the interaction of nucleobases with alkaline and alkaline earth metal cations: A density functional theory investigation. *J. Phys. Chem. A* **2004**, *108*, 4008–4018.

(19) Zins, E.-L.; Rochut, S.; Pepe, C. Theoretical and experimental studies of cationized uracil complexes in the gas phase. *J. Mass Spectrom.* **2009**, *44*, 40–49.

(20) Krasnokutski, S. A.; Lee, J. S.; Yang, D.-S. High-resolution electron spectroscopy and structures of lithium-nucleobase (adenine, uracil, and thymine) complexes. *J. Chem. Phys.* **2010**, *132*, 044304.

(21) Davis, J. T. G-quartets 40 years later: from 5'-GMP to molecular biology and supramolecular chemistry. *Angew. Chem., Int. Ed.* **2004**, *43*, 668–698.

(22) Ciesielski, A.; Lena, S.; Masiero, S.; Spada, G. P.; Samori, P. Dynamers at the solid-liquid interface: controlling the reversible assembly/reassembly process between two highly ordered supramolecular guanine motifs. *Angew. Chem., Int. Ed.* **2010**, *49*, 1963–1966.

(23) Xu, W.; Tan, Q.; Yu, M.; Sun, Q.; Kong, H.; Lægsgaard, E.; Stensgaard, I.; Kjems, J.; Wang, J.-G.; Wang, C.; Besenbacher, F. Atomic-scale structures and interactions between the guanine quartet and potassium. *Chem. Commun.* **2013**, *49*, 7210–7212.

(24) Zhang, C.; Wang, L.; Xie, L.; Kong, H.; Tan, Q.; Cai, L.; Sun, Q.; Xu, W. Solventless formation of G-quartet complexes based on alkali and alkaline earth salts on Au(111). *ChemPhysChem* **2015**, *16*, 2099–2105.

(25) Gonzalez-Rodriguez, D.; Janssen, P. G. A.; Martin-Rapun, R.; Cat, I. D.; Feyter, S. D.; Schenning, A. P. H. J.; Meijer, E. W. Persistent, well-defined, monodisperse, pi-conjugated organic nanoparticles via G-quadruplex self-assembly. *J. Am. Chem. Soc.* **2010**, *132*, 4710–4719.

(26) Qiu, B.; Liu, J.; Qin, Z.; Wang, G.; Luo, H. Quintets of uracil and thymine: a novel structure of nucleobase self-assembly studied by electrospray ionization mass spectrometry. *Chem. Commun.* **2009**, *20*, 2863–2865.

(27) Ding, Y.; Wang, X.; Xie, L.; Yao, X.; Xu, W. Two-dimensional self-assembled nanostructures of nucleobases and their related derivatives on Au(111). *Chem. Commun.* **2018**, *54*, 9259–9269.

(28) Wang, X.; Xie, L.; Ding, Y.; Yao, X.; Zhang, C.; Kong, H.; Wang, L.; Xu, W. Interactions between Bases and Metals on Au(111)

under Ultrahigh Vacuum Conditions. *Acta Phys. -Chim. Sin.* **2018**, *34*, 1321–1333.

(29) Besenbacher, F. Scanning tunnelling microscopy studies of metal surfaces. *Rep. Prog. Phys.* **1996**, *59*, 1737–1802.

(30) Lægsgaard, E.; Østerlund, L.; Thostrup, P.; Rasmussen, P. B.; Stensgaard, I.; Besenbacher, F. A high-pressure scanning tunneling microscope. *Rev. Sci. Instrum.* **2001**, *72*, 3537–3542.

(31) Kresse, G.; Hafner, J. Ab initio molecular dynamics for open-shell transition metals. *Phys. Rev. B: Condens. Matter Mater. Phys.* **1993**, *48*, 13115–13118.

(32) Kresse, G.; Furthmüller, J. Efficient iterative schemes for ab initio total-energy calculations using a plane-wave basis set. *Phys. Rev. B: Condens. Matter Mater. Phys.* **1996**, *54*, 11169–11186.

(33) Blöchl, P. E. Projector augmented-wave method. *Phys. Rev. B: Condens. Matter Mater. Phys.* **1994**, *50*, 17953–17979.

(34) Kresse, G.; Joubert, D. From ultrasoft pseudopotentials to the projector augmented-wave method. *Phys. Rev. B: Condens. Matter Mater. Phys.* **1999**, *59*, 1758–1775.

(35) Perdew, J. P.; Burke, K.; Ernzerhof, M. Generalized gradient approximation made simple. *Phys. Rev. Lett.* **1996**, *77*, 3865–3868.

(36) Grimme, S.; Antony, J.; Ehrlich, S.; Krieg, H. A consistent and accurate ab initio parametrization of density functional dispersion correction (DFT-D) for the 94 elements H-Pu. *J. Chem. Phys.* **2010**, *132*, 154104.

(37) Tersoff, J.; Hamann, D. R. Theory of the scanning tunneling microscope. *Phys. Rev. B: Condens. Matter Mater. Phys.* **1985**, *31*, 805–813.

(38) Vanpoucke, D. E. P.; Brocks, G. Formation of Pt-induced Ge atomic nanowires on Pt/Ge(001): A density functional theory study. *Phys. Rev. B: Condens. Matter Mater. Phys.* **2008**, *77*, 241308.

(39) Sowerby, S. J.; Petersen, G. B. Scanning tunneling microscopy of uracil monolayers self-assembled at the solid/liquid interface. *J. Electroanal. Chem.* **1997**, *433*, 85–90.

(40) Dretschkow, T.; Dakkouri, A. S.; Wandlowski, T. In-situ scanning tunneling microscopy study of uracil on Au(111) and Au(100). *Langmuir* **1997**, *13*, 2843–2856.

(41) Wang, X.; Ding, Y.; Li, D.; Xie, L.; Xu, W. Linear array of cesium atoms assisted by uracil molecules on Au(111). *Chem. Commun.* **2019**, *55*, 12064–12067.